Rapid Formation of Secondary Organic Aerosol from the Photolysis of 1-Nitronaphthalene: Role of Naphthoxy Radical Self-reaction

ARTICLE *in* ENVIRONMENTAL SCIENCE & TECHNOLOGY · SEPTEMBER 2012

Impact Factor: 5.33 · DOI: 10.1021/es302841j

6 AUTHORS, INCLUDING:

Robert Healy
Ontario Ministry of the Environment
38 PUBLICATIONS **425** CITATIONS
SEE PROFILE

Yang Chen
University College Cork
3 PUBLICATIONS **27** CITATIONS
SEE PROFILE

Ivan Kourtchev
University of Cambridge
44 PUBLICATIONS **1,432** CITATIONS
SEE PROFILE

John C Wenger
University College Cork
125 PUBLICATIONS **2,362** CITATIONS
SEE PROFILE

Environmental Science & Technology

Article

pubs.acs.org/est

Rapid Formation of Secondary Organic Aerosol from the Photolysis of 1-Nitronaphthalene: Role of Naphthoxy Radical Self-reaction

Robert M. Healy,*[,†] Yang Chen,[†] Ivan Kourtchev,[‡] Markus Kalberer,[‡] Deborah O'Shea,[†] and John C. Wenger[†]

[†]Department of Chemistry and Environmental Research Institute, University College Cork, Ireland

[‡]Department of Chemistry, University of Cambridge, Lensfield Road, Cambridge,CB2 1EW, U.K.

Supporting Information

ABSTRACT: The chemical composition of secondary organic aerosol (SOA) formed from the photolysis of 1-nitronaphthalene in a series of simulation chamber experiments has been investigated using an aerosol time-of-flight mass spectrometer (ATOFMS). The resulting SOA is characterized by the presence of a dimer (286 Da) proposed to be formed through the self-reaction of naphthoxy radicals along with the expected product nitronaphthol. The molecular formulas of the SOA products were confirmed by collecting filter samples and analyzing the extracts using ultrahigh resolution mass spectrometry. Further evidence for the radical self-reaction mechanism was obtained by photolyzing 1-nitronaphthalene in the presence of excess nitrobenzene, where it was shown that the resulting SOA contained a product consistent with the cross-reaction of phenoxy and naphthoxy radicals. The naphthoxy dimer was formed from the photolysis of 1-nitronaphthalene under a variety of different experimental conditions including the presence of excess butyl ether as an OH scavenger and the presence of ambient air and particles. However, formation of the dimer was suppressed when 1-nitronaphthalene was photolyzed in the presence of excess NO and nitronaphthol was instead found to be the dominant particle-phase product indicating that the yield of the dimer is dependent upon the concentration of pre-existing NO_x. The results of this work suggest that photolysis of 1-nitronaphthalene represents a previously unidentified pathway to SOA formation in the troposphere. Analogous mechanisms may also be important for other nitrated polycyclic aromatic hydrocarbons.

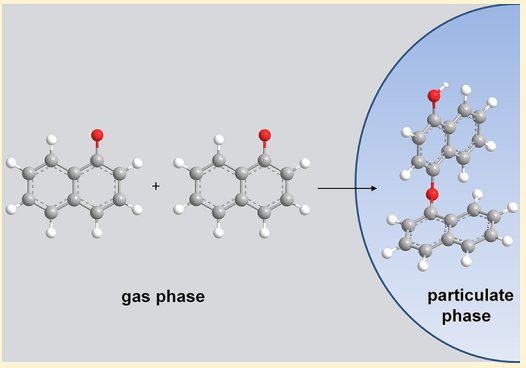

INTRODUCTION

Nitrated polycyclic aromatic hydrocarbons (nitro-PAHs) are of concern from a human health perspective due to their known mutagenic and carcinogenic effects.[1−5] Nitro-PAHs can be emitted directly through combustion processes, most notably gasoline and diesel engines,[6−9] but can also be formed through the reaction of PAHs with the hydroxyl or nitrate radical in the presence of NO_x.[2,10−16] In ambient air, nitronaphthalenes are detected predominantly in the gas phase, nitroanthracenes are found in both gas and particulate phases, and larger nitro-PAHs such as nitropyrenes are observed predominantly in the particulate phase.[9,17−23] The most abundant gas-phase nitro-PAHs typically detected are 1- and 2-nitronaphthalene.[9,17] Detailed gas-phase degradation mechanisms are required for these compounds to better understand their potential contribution to air quality and, in particular, secondary organic aerosol (SOA) formation.

Gas-phase photolysis has been determined to be the major degradation pathway for 1-nitronaphthalene (1NN) under ambient conditions with a lifetime with respect to photolysis estimated at ≤1 h.[24−27] The photolysis of nitro-PAHs is believed to lead to the formation of nitric oxide and an aryloxy radical,[28−30] which can undergo further reaction to yield products such as quinones, hydroxy-PAHs, and hydroxynitro-PAHs.[31−33] The observed formation of 1,4-naphthoquinone and 2-nitro-1-naphthol as products of the gas-phase photolysis of 1NN is also consistent with a mechanism involving the formation of naphthoxy radicals through photodissociation.[24] 4-Nitro-1-naphthol has also been detected in high-NOx naphthalene photooxidation experiments and proposed to be formed through the reaction of 1NN with OH;[34] however, photolysis may also have contributed to its formation in that case.

The aim of this work was to investigate the chemical composition of SOA formed from the photolysis of 1NN in a series of simulation chamber experiments performed under a variety of experimental conditions. Online aerosol mass spectrometry and off-line ultrahigh resolution mass spectrometry were used to characterize the aerosol formed.

EXPERIMENTAL SECTION

All experiments were performed in the 3.91 m^3 atmospheric simulation chamber at University College Cork, described in

Received: July 13, 2012
Revised: September 13, 2012
Accepted: September 26, 2012
Published: September 26, 2012

dx.doi.org/10.1021/es302841j | Environ. Sci. Technol. 2012, 46, 11813−11820

detail elsewhere.[35] Briefly, the chamber is cylindrical in shape, made of FEP foil, and closed at both ends by FEP foil covered plates. The chamber is surrounded by 16 Philips TL12 (40 W) lamps with an emission maximum at 310 nm and 12 Philips TL05 (40 W) lamps with an emission maximum at 360 nm (Figure S1 of the Supporting Information) delivering a light intensity equivalent to $j(NO_2) = 6.6 \times 10^{-3}$ s^{-1}. The chamber and lamps are surrounded by a housing consisting of aluminum profiles and sheets. Dry air is generated using an air purification system (Zander KMA 75), which reduces concentrations of NO_x and nonmethane hydrocarbons to <10 ppbv. The temperature and amount of water in the chamber is monitored by a dew point meter (Vaisala DM70). The relative humidity in the chamber was typically less than 1%. Experiments were performed at ambient temperature (295 ± 2 K) and atmospheric pressure. The background concentration of particles in the chamber was <200 cm^{-3} with the exception of one experiment where ambient air and particles were introduced purposefully. 1NN was introduced by slowly heating the compound in an impinger using a gentle flow of purified air. Sample introduction lasted approximately 15 min. The starting concentration of 1NN for all of the experiments described here was approximately 150 ppbv and all of the lamps were used for photolysis. A scanning mobility particle sizer (TSI model 3081) was used to measure particle number-size distributions in the range 11−478 nm (mobility diameter, d_m) every 3 min. NO_x and O_3 analyzers (Thermo Model 42*i* and 49*i*, respectively) were also available for experiment A.

Five experiments were performed under different experimental conditions as shown in Table 1. The details of these experiments were as follows: A: 1NN photolysis. B: 1NN photolysis in the presence of butyl ether. Approximately 10 ppmv butyl ether was introduced to minimize the reaction of background OH radicals with 1NN.[36] C: 1NN photolysis in the presence of nitrobenzene (NB). Approximately 10 ppmv NB was used to investigate the reaction of naphthoxy and phenoxy radicals. The photolysis rate of NB ($\sim 1 \times 10^{-5}$ s^{-1})[37] is much lower than 1NN (1.37×10^{-4} s^{-1})[24] and thus an excess of the former was required. D: 1NN photolysis in the presence of 800 ppbv NO. A relatively high concentration of NO was used in an attempt to suppress naphthoxy radical self-reaction.[28] E: 1NN photolysis in the presence of ambient air. The chamber was filled with laboratory air to investigate whether the naphthoxy radical self-reaction would proceed under these conditions. The resulting particle mass concentration was approximately 2 μg m^{-3} (11−478 nm, assuming a density of 1.4 g cm^{-3}), NO and NO_x concentrations were 0 and 8 ppbv respectively.

Table 1. Experimental Conditions for the Photolysis Experiments, 150 ppbv 1-Nitronaphthalene (1NN) was Introduced in each Case

experiment	experimental conditions	purpose
A	1NN photolysis	investigate SOA composition
B	1NN + 10 ppmv butyl ether	scavenge OH radicals
C	1NN + 10 ppmv nitrobenzene	investigate naphthoxy-phenoxy reaction
D	1NN + 800 ppbv NO	suppress dimer formation
E	1NN + ambient air	investigate dimer formation in ambient air

An aerosol time-of-flight mass spectrometer (ATOFMS, TSI model 3800) fitted with an aerodynamic lens (TSI model AFL100) was used to investigate the chemical composition of the SOA formed. The instrument is described in detail elsewhere.[38] Briefly, single particles are sampled through a critical orifice and focused into a tight beam in the aerodynamic lens before transmission to the sizing region. Here, the aerodynamic diameter (d_{va}) of each particle is calculated based on its time-of-flight between two continuous wave lasers (Nd:YAG, 532 nm). The velocity of each particle is used to calculate its time of arrival in the ionization region of the instrument where desorption/ionization is performed using a Nd:YAG laser (266 nm). The resulting positive and negative ions are analyzed simultaneously using a bipolar time-of-flight mass spectrometer. Typically, the Nd:YAG laser is operated using a laser energy of approximately 1 mJ per pulse; however, lower pulse energies were employed in this work in order to minimize fragmentation as described in the next section.

Filter samples were also collected for selected experiments. Air from the chamber was drawn through prebaked quartz fiber filters at 5 L min^{-1} for 40 min. Blank filters were prepared by pumping air from the chamber using the same conditions before the addition of the reactants. One blank filter was collected for each experiment and blank filter signals ranged from 25 to 17 000 times lower than product filter signals for the m/z values selected for product identification. One quarter of each filter was extracted in 2.5 mL methanol-acetonitrile (3:1 v/v) for 50 min under ultrasonic agitation. The extracts were then reduced to a volume of approximately 400 μL under a gentle stream of N_2 and 100 μL of water was finally added to each extract. The final extracts were analyzed using an ultrahigh resolution LTQ Orbitrap Velos mass spectrometer (Thermo Fisher, Bremen, Germany) equipped with a TriVersa Nanomate robotic nanoflow chip-based electrospray ionization (ESI) source (Advion Biosciences, Ithaca NY, USA). The ion source was controlled by *Chipsoft 8.3.1* software (Advion Biosciences). The ionization voltage was +1.4 kV in positive mode and −1.4 kV in negative mode. The backpressure was set at 0.8 psi in both modes. The LTQ Orbitrap mass resolution was 100 000 at m/z 400. The positive ion mass spectra were found to be too noisy and thus only the negative ion mass spectra are discussed here.

RESULTS AND DISCUSSION

The direct photolysis of 1NN in the simulation chamber resulted in rapid SOA formation as shown in Figure 1. Nucleation occurs within 3 min, the time required to perform the first SMPS scan, and the particle number concentration reaches a maximum within 20 min. Although the ATOFMS has a lower sizing limit of approximately 150 nm (d_{va}), the majority of the SOA size distribution lies within the range of detection. The SOA composition was homogeneous across the size range detected and is expected to be homogeneous across the entire size distribution. The mass spectra of the SOA were dominated by organic fragment ions when the Nd:YAG laser was operated at a laser pulse energy of 1 mJ. Thus, the laser pulse energy was reduced in steps to investigate the effect upon the resultant dual ion mass spectra. The effect of reducing the laser pulse energy is shown in Figure 2. Because of inhomogeneous laser power density across the laser beam that interacts with the particles, the power density associated with each mass spectrum generated is difficult to calculate accurately and can potentially vary within an order of magnitude.[39] Thus, only the laser pulse energy used is reported here.

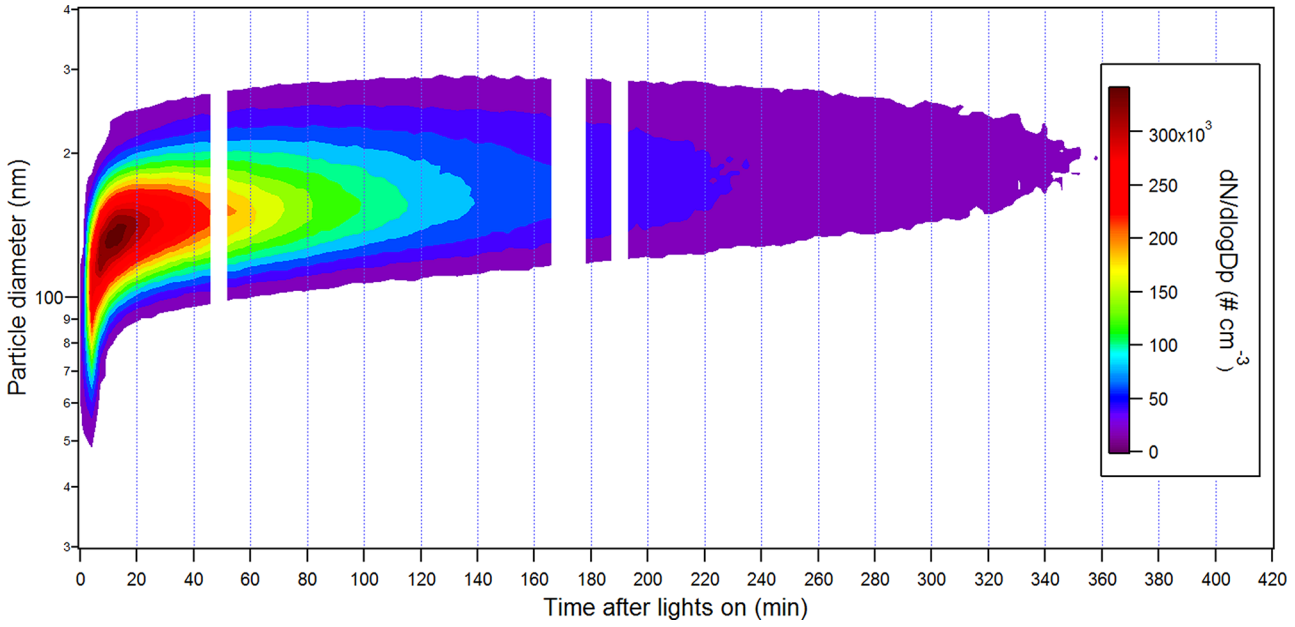

Figure 1. Number-size distribution of SOA formed from the photolysis of 1-nitronaphthalene in experiment A (not corrected for wall loss).

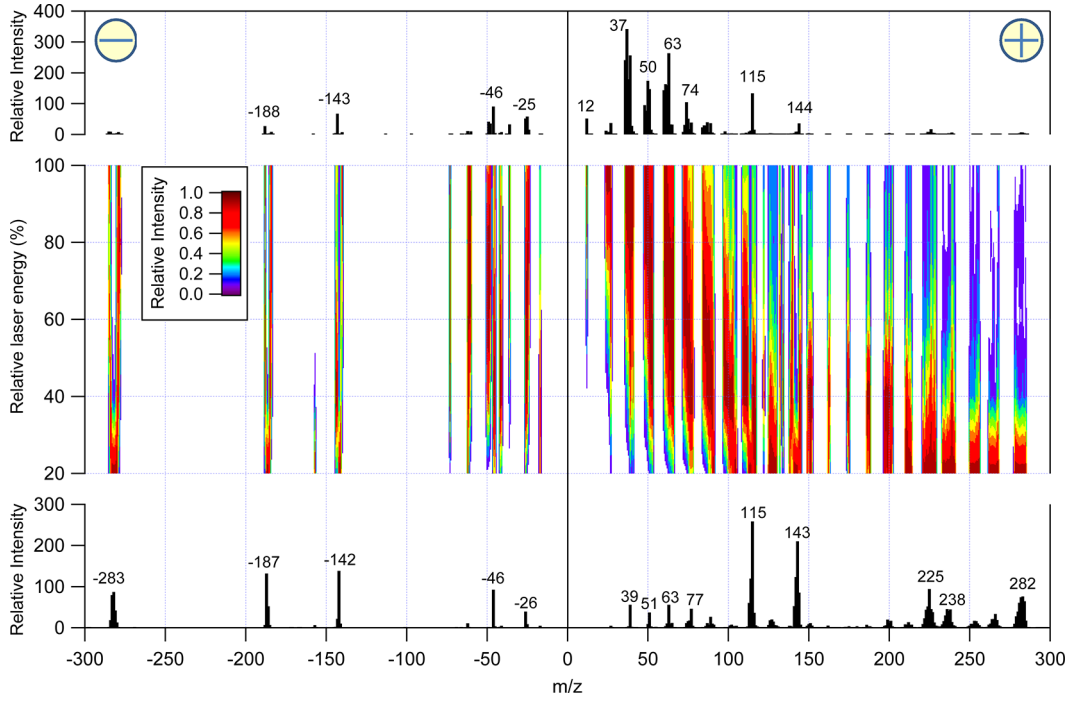

Figure 2. Top panel: Average dual ion mass spectrum of SOA generated from the photolysis of 1-nitronaphthalene using a desorption/ionization laser pulse energy of 1 mJ. Middle panel: Effect of decreasing the desorption/ionization laser pulse energy in 0.2 mJ steps from 1 to 0.2 mJ upon the average dual ion mass spectra. The color scale corresponds to the relative intensity of the ions normalized to 1 for each m/z. Bottom panel: Average dual ion mass spectrum obtained using a desorption/ionization laser pulse energy of 0.2 mJ. The number of mass spectra averaged for laser energies of 1, 0.8, 0.6, 0.4, and 0.2 mJ were 1360, 860, 670, 540, and 960, respectively.

Using a laser pulse energy of 1 mJ results in an average mass spectrum dominated by fragment ions (top panel of Figure 2). In the positive ion mass spectrum, characteristic ions include m/z 12 $(C)^+$, 37 $(C_3H)^+$, 50 $(C_4H_2)^+$, 63 $(C_5H_3)^+$, 74 $(C_6H_2)^+$, 115 $(C_9H_7)^+$, and 144 $(C_{10}H_8O)^+$. Whereas the smaller ions are less useful for product identification, m/z 115 can be considered as a diagnostic fragmentation ion for substituted naphthalenes. In the negative ion mass spectrum m/z −25 $(C_2H)^-$, −46 $(NO_2)^-$, −143 $(C_{10}H_7O)^-$, and −188 $(C_{10}H_6NO_3)^-$ are observed. Deprotonated ions are commonly observed for carboxylic and hydroxyl-containing organic compounds using laser desorption/ionization mass spectrometry[40,41] and the ion at m/z −188 is therefore assigned to nitronaphthol $(M\text{-}H)^-$. This assignment is confirmed using ultrahigh resolution mass spectrometry as described below.

As shown in Figure 2 (middle panel), when the laser energy is reduced in 0.2 mJ steps, the relative intensity of the smaller hydrocarbon fragment ions decreases significantly, whereas the

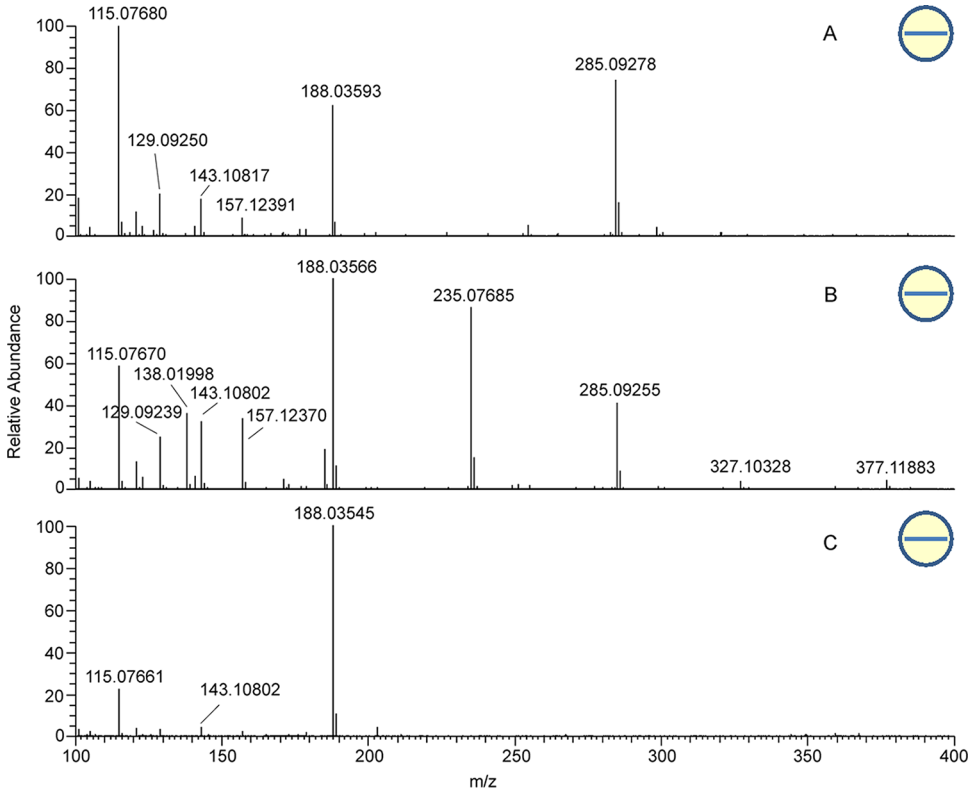

Figure 3. Ultrahigh resolution mass spectrum (negative ion mode) for SOA formed from the photolysis of 1-nitronaphthalene (1NN) under different experimental conditions. A: 1NN photolysis. B: 1NN photolysis in the presence of excess nitrobenzene. C: 1NN photolysis in the presence of excess NO.

signal for the larger ions increases. This effect has been observed in previous single particle desorption/ionization mass spectrometry studies.[39,40,42,43] The smaller hydrocarbon fragment ions formed at lower laser pulse energies are also quite different (bottom panel of Figure 2). Peaks are observed at m/z 39 $(C_3H_3)^+$, 51 $(C_2H_3)^+$, 63 $(C_5H_3)^+$, and 77 $(C_6H_5)^+$, corresponding to well-established aromatic fragment ions.[44] Interestingly, although the signal intensities observed at higher m/z values increase, ions are observed possessing shifted m/z values. In the positive ion mass spectra m/z 144 is replaced with 143 $(C_{10}H_7O)^+$ and in the negative ion mass spectra m/z −143 is partly replaced by −142 $(C_{10}H_6O)^-$ and m/z −188 is significantly replaced with −187 $(C_{10}H_5NO_3)^-$. Fragmentation involving the loss of two hydrogen atoms may explain the observation of these ions.

At 0.2 mJ, new clusters of ions are observed between m/z −280 and −285 in the negative ion mass spectrum and between m/z 279 and 286 in the positive ion mass spectrum. Ions are also observed in the m/z ranges 221−227, 232−240, and 261−268 in the positive ion mass spectrum. The smaller clusters, and the ions observed at m/z −143, −142, and 143 may represent fragment ions of a larger molecule. Products with such high molecular masses are not expected based on the existing mechanisms for the gas-phase photolysis of 1NN.[24,27] The broad clusters of ions observed by ATOFMS preclude accurate identification of the molecular formula of this product and therefore ultrahigh resolution ESI-LTQ Orbitrap mass spectrometry with a mass accuracy power <1.5 ppm was used for confirmation. The average ultrahigh resolution mass spectrum of SOA formed from the photolysis of 1NN is given in part A of Figure 3. The largest peak is observed at m/z −115.0768 and corresponds to the $(C_9H_7)^-$ fragment ion associated with substituted naphthalenes. Although this fragment was detected as a positive ion by ATOFMS, the presence of a positive ion could not be confirmed for the Orbitrap data. The second-highest peak is observed at m/z −285.09278 $(C_{20}H_{13}O_2)$. Peaks observed in the negative ion mode often represent deprotonated products, and thus a likely molecular mass for this product is 286.09938 Da $(C_{20}H_{14}O_2)$. This molecular formula is consistent with a naphthoxy radical dimer. The ATOFMS and the ESI-Orbitrap utilize entirely different ionization techniques and thus it seems unlikely that this dimer is an ionization artifact. A peak is also observed at m/z −188.03593, corresponding to deprotonated nitronaphthol, in agreement with the ATOFMS data. It is not possible to identify which isomers are formed for these products based on their molecular formulas alone. MS/MS analysis was also performed to confirm the identity of nitronaphthol and the naphthoxy dimer as reaction products (Figure S2 and S3 of the Supporting Information).

The two potential 1NN photolysis mechanisms that are expected to result in the formation of naphthoxy radicals are given in Scheme 1. The nitro−nitrite rearrangement has been proposed to arise from an n,π^* excited state for anthroxy and pyroxy radicals.[28,32,45] This species can either undergo an intramolecular rearrangement through an oxaziridene intermediate to form the nitrite or dissociate to form nitrogen dioxide and a naphthyl radical, which then recombine to form the nitrite. The intramolecular rearrangement is most favorable for nitro-PAHs with 2 *peri*-hydrogens, for example 9-nitroanthracene, because the nitro group is sterically twisted out of the plane of the aromatic ring. This results in overlap of the

Scheme 1. Mechanisms for the Photolysis of 1-Nitronaphthalene Resulting in the Formation of the Naphthoxy Radical and Nitric Oxide, Adapted from Chapman et al.[28]

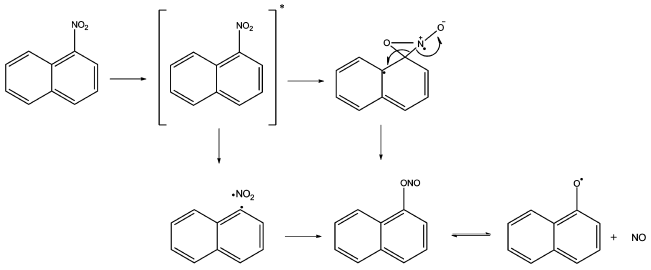

half-vacant nonbonding orbital of the nitro group with the adjacent orbital of the aromatic ring, thus facilitating the formation of the oxaziridene intermediate.[28] 1NN does not possess two *peri*-hydrogens and thus the nitro group is oriented in the same plane as the aromatic ring.[46] Therefore, 1NN is more stable with respect to photolysis than 9-nitroanthracene.[28] It is not possible to identify which of the two mechanisms leads to the formation of the naphthoxy radical in this work. Confirmation of the dominant mechanism for 1NN, and the analogous mechanism for 1-nitropyrene, has proved challenging.[29,30] Scission of the CN bond to form an aryl radical and NO_2 without rearrangement, thus resulting in the subsequent formation of aryl peroxy radicals and NO_2, is a pathway that has been observed for nitrobenzene at wavelengths lower than 280 nm.[47] However, this pathway is unlikely to be important at the wavelengths employed in this work. Furthermore, NO was observed as a primary photolysis product in experiment A, whereas the mixing ratio of NO_2 increased much later in the experiment through oxidation of NO (Figure S4 of the Supporting Information). This observation supports the mechanism provided in Scheme 1.

To the best of our knowledge, there have been no previous reports of the naphthoxy radical self-reaction in the literature. The self-reaction of phenoxy radicals, generated through the reaction of Cl atoms with phenol, to form dimers has been previously reported.[48,49] Although it could not be ascertained whether the dimers formed existed in the gas or particulate phase, the major product identified was 4-phenoxyphenol, whereas other isomers were also formed in smaller quantities. Potential structures for those isomers included biphenol and diphenylperoxide, although the latter was disregarded as it was not estimated to be a thermodynamically stable product. The phenoxy radical has been previously determined to be very stable with respect to reaction with O_2, most likely due to its strong resonance stabilization,[48] and thus reactions with NO and NO_2 have been proposed as the major degradation pathways under ambient conditions. More recently, reaction of phenoxy with the hydroperoxyl radical has been identified as another potentially important degradation pathway.[50]

Although dimers have not been previously reported as a product of 1NN photolysis, a previous study focused on the photolysis of 9-nitroanthracene in acetone solution did result in the formation of bianthrone. This product was proposed to have formed through the self-reaction of 9-anthryloxy radicals.[28] The expected self-reaction of naphthoxy radicals to produce dimers is shown in Scheme 2. The potential structures are analogous to those previously observed from the self-reaction of phenoxy and anthroxy radicals.[28,49] To investigate

Scheme 2. Proposed Self-Reaction of Naphthoxy Radicals to Form Dimers. Note that Structural Isomers of the Three Potential Dimer Structures are also Possible Products

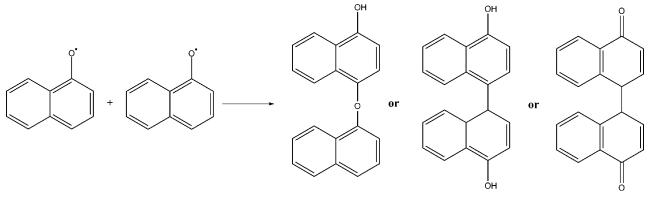

the formation of these dimers, several experiments were performed under different experimental conditions. The ATOFMS mass spectra of the SOA formed in these experiments are given in parts A–E of Figure 4. Dimers were successfully formed both in the absence (part A of Figure 4) and presence of 10 ppmv butyl ether (part B of Figure 4) suggesting that background levels of OH radicals that may be present in the chamber are not responsible for dimer formation.

To confirm the role of aryloxy radicals in the production of these dimers, 1NN was photolyzed in the presence of excess nitrobenzene. The photolysis of nitrobenzene is a source of phenoxy radicals, and dimers were formed that are consistent with the cross-reaction of phenoxy and naphthoxy radicals (236 Da), as shown in part C of Figure 4 (m/z 235). The possible structures of the phenoxy–naphthoxy dimers are shown in Scheme 3. The molecular formula of the dimer was confirmed using ultrahigh resolution mass spectrometry. As shown in part B of Figure 3, the mass spectrum is characterized by an additional intense peak at m/z −235.07685 ($C_{16}H_{11}O_2$), consistent with the deprotonated phenoxy-naphthoxy dimer. Interestingly, a small peak is also observed at m/z −377.11883, which is consistent with a deprotonated trimer potentially formed from the reaction of naphthoxy with a neutral naphthol molecule, followed by a termination step with a phenoxy radical, or the reverse order. A smaller peak is also observed at m/z −327.10328, possibly arising from a similar propagation reaction involving phenol as the neutral molecule.

When 1NN was photolyzed in the presence of 800 ppbv NO however, the signal for ions associated with the dimer in the ATOFMS mass spectra were either absent or greatly reduced in intensity (part D of Figure 4). Instead, an intense signal was observed for nitronaphthol at m/z −187, indicating that dimer formation can be suppressed through the reaction of naphthoxy and NO_x, a pathway that has previously been confirmed for pyroxy and anthroxy radicals in solution,[28,32] and phenoxy radicals in the gas phase.[49] 2-Nitro-1-naphthol was previously detected as a product in the gas-phase photolysis of 1NN by Atkinson et al.;[24] however, no mechanism was proposed for its formation. Here, it is proposed that nitronaphthol may be formed through the reaction of NO_2 with the naphthoxy radical as shown in Figure S5 of the Supporting Information. This product has also been observed during a chamber study of the photooxidation of naphthalene where it has been demonstrated to partition predominantly to the particulate phase.[34] The significant changes in SOA composition detected by ATOFMS during this experiment are also apparent in the ultrahigh resolution mass spectrum, shown in part C of Figure 3. Peaks associated with the dimer are absent or significantly reduce in intensity and the spectrum is characterized by a base peak corresponding to deprotonated nitronaphthol at m/z −188.03545. Although an additional cluster of ions is observed at m/z 291–298 in the ATOFMS average mass spectrum (part

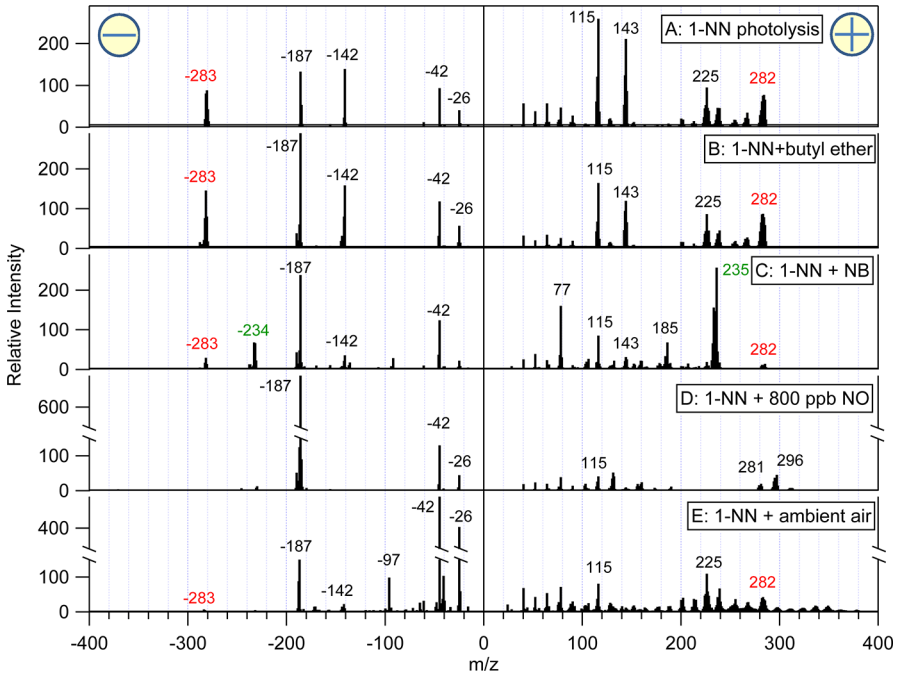

Figure 4. Average dual ion mass spectra obtained from SOA formed from the photolysis of 150 ppb 1-nitronaphthalene (1NN) under different experimental conditions. A: Photolysis. B: in the presence of excess butyl ether. C: in the presence of excess nitrobenzene. D: in the presence of excess NO. E: in the presence of background ambient air and particles. Red text denotes ions associated with the naphthoxy dimer and green text denotes ions associated with the naphthoxy-phenoxy dimer. The number of mass spectra averaged for experiments A–E were 960, 3970, 3620, 2360, and 5420, respectively.

Scheme 3Proposed Reaction of Naphthoxy and Phenoxy Radicals to Form Dimers. Note that Structural Isomers of the Three Potential Dimer Structures are also Possible Products

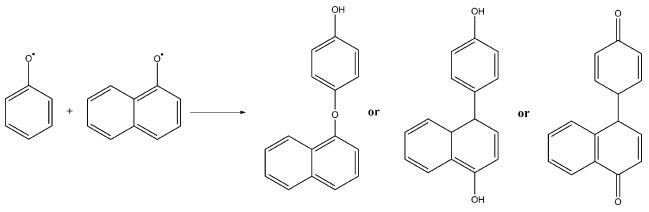

D of Figure 4), there is no corresponding species observed in the ultrahigh resolution mass spectrum precluding the identification of this product.

Finally, 1NN was photolyzed in the presence of ambient air and particles to investigate whether the naphthoxy radical self-reaction would be relevant under these conditions. The average mass spectrum for the ambient particles before irradiation is shown in Figure S6 of the Supporting Information and is characteristic of typical aged urban combustion aerosol observed in the local environment.[51] The pre-existing NO and NO_x concentrations were relatively low, 0 and 8 ppbv, respectively. The average ATOFMS mass spectrum after the lamps were switched on is shown in part E of Figure 4. There are some additional peaks that were not observed in the previous experiments. The negative ion mass spectrum is characterized by intense peaks at m/z −26 $(CN)^-$, −42 $(CNO)^-$, and −97 $(HSO_4)^-$, consistent with nitrogen-containing organics and sulfate, species that are routinely detected in ambient particles.[38,42] There is also evidence of some unidentified high molecular weight products in the range m/z 300–360 in the positive ion mass spectrum. The formation of naphthoxy dimers is confirmed by the presence of peaks at m/z 225, 282, and −283, although the intensity of the signals is lower relative to those observed in parts A and B of Figure 4 suggesting competing pathways for naphthoxy radicals.

The direct photolysis of volatile organic compounds is typically not recognized as a source of SOA in the atmosphere. However, recent studies have shown that photolysis of nitrophenols[52] and aromatic aldehydes[53] can produce SOA and the results of this work indicate that similar investigations into other substituted aromatics are warranted. The SOA formed from the photolysis of 1NN contains nitronaphthol and a dimer arising from the self-reaction of naphthoxy radicals. The unexpected observation of the latter species suggests that the self-reaction and cross-reactions of aryloxy radicals may represent a potential pathway to SOA formation. However, competing reactions with NO, NO_2, and potentially the hydroperoxyl radical[50] are likely to suppress dimer formation in the atmosphere. Further, more detailed work is required to investigate the relative importance of these reaction pathways. The effect of relative humidity should also be explored considering the potential for 1NN to form radical species in solution when irradiated.[54−56] Despite its short atmospheric lifetime with respect to photolysis, daytime 1NN concentrations of up to 2 ng m^{-3} have been measured in Southern California during photochemical pollution episodes.[56−58] The photolysis of 1NN, typically the most abundant gas-phase nitro-PAH measured in ambient air, may thus represent a previously unreported source of SOA in urban areas. The SOA yields and kinetics for the photolysis of 1NN under natural sunlight conditions will be reported in a future publication.

■ ASSOCIATED CONTENT

Supporting Information

This includes lamp emission spectra, MS/MS analysis results, trace gas, and particle mass concentration profiles for experiment A, a mechanism for the formation of nitronaphthol and an average mass spectrum of ambient particles for experiment E. This material is available free of charge via the Internet at http://pubs.acs.org.

■ AUTHOR INFORMATION

Corresponding Author

*E-mail: robert.healy@ucc.ie.

Notes

The authors declare no competing financial interest.

■ ACKNOWLEDGMENTS

This work was supported by the European Commission through the research project EUROCHAMP 2 (contract number 228355) and the Irish Environmental Protection Agency STRIVE Programme (project 2008-PhD-AQ-1). The work at the University of Cambridge was supported by Marie Curie FP7-PEOPLE-2009-IEF (Project number 254319).

■ REFERENCES

(1) Tokiwa, H.; Ohnishi, Y. Mutagenicity and carcinogenicity of nitroarenes and their sources in the environment. *Crit. Rev. Toxicol.* **1986**, *17* (1), 23−60.

(2) Atkinson, R.; Arey, J. Atmospheric chemistry of gas-phase polycyclic aromatic hydrocarbons: formation of atmospheric mutagens. *Environ. Health Perspect.* **1994**, *102*, 117−126.

(3) Finlayson-Pitts, B. J.; Pitts, J. N. Tropospheric air pollution: Ozone, airborne toxics, polycyclic aromatic hydrocarbons, and particles. *Science* **1997**, *276* (5315), 1045−1051.

(4) Øvrevik, J.; Arlt, V. M.; Øya, E.; Nagy, E.; Mollerup, S.; Phillips, D. H.; Låg, M.; Holme, J. A. Differential effects of nitro-PAHs and amino-PAHs on cytokine and chemokine responses in human bronchial epithelial BEAS-2B cells. *Toxicol. Appl. Pharmacol.* **2010**, *242* (3), 270−280.

(5) Landvik, N. E.; Gorria, M.; Arlt, V. M.; Asare, N.; Solhaug, A.; Lagadic-Gossmann, D.; Holme, J. A. Effects of nitrated-polycyclic aromatic hydrocarbons and diesel exhaust particle extracts on cell signalling related to apoptosis: Possible implications for their mutagenic and carcinogenic effects. *Toxicology* **2007**, *231* (2−3), 159−174.

(6) Paputa-Peck, M. C.; Marano, R. S.; Schuetzle, D.; Riley, T. L.; Hampton, C. V.; Prater, T. J.; Skewes, L. M.; Jensen, T. E.; Ruehle, P. H. Determination of nitrated polynuclear aromatic hydrocarbons in particulate extracts by using capillary column gas chromatography with nitrogen selective detection. *Anal. Chem.* **1983**, *55* (12), 1946−1954.

(7) MacCrehan, W. A.; May, W. E.; Yang, S. D.; Benner, B. A. Determination of nitro-polynuclear aromatic hydrocarbons in air and diesel particulate matter using liquid chromatography with electrochemical and fluorescence detection. *Anal. Chem.* **1988**, *60* (3), 194−199.

(8) Carrara, M.; Wolf, J.-C.; Niessner, R. Nitro-PAH formation studied by interacting artificially PAH-coated soot aerosol with NO_2 in the temperature range of 295−523 K. *Atmos. Environ.* **2010**, *44* (32), 3878−3885.

(9) Albinet, A.; Leoz-Garziandia, E.; Budzinski, H.; Villenave, E. Polycyclic aromatic hydrocarbons (PAHs), nitrated PAHs and oxygenated PAHs in ambient air of the Marseilles area (South of France): Concentrations and sources. *Sci. Total Environ.* **2007**, *384* (1−3), 280−292.

(10) Ramdahl, T.; Zielinska, B.; Arey, J.; Atkinson, R.; Winer, A. M.; Pitts, J. N. Ubiquitous occurrence of 2-nitrofluoranthene and 2-nitropyrene in air. *Nature* **1986**, *321* (6068), 425−427.

(11) Arey, J.; Zielinska, B.; Atkinson, R.; Winer, A. M.; Ramdahl, T.; Pitts, J. N., Jr The formation of nitro-PAH from the gas-phase reactions of fluoranthene and pyrene with the OH radical in the presence of NO_x. *Atmos. Environ.* **1986**, *20* (12), 2339−2345.

(12) Zielinska, B.; Arey, J.; Atkinson, R.; McElroy, P. A. Nitration of acephenanthrylene under simulated atmospheric conditions and in solution and the presence of nitroacephenanthrylene(s) in ambient particles. *Environ. Sci. Technol.* **1988**, *22* (9), 1044−1048.

(13) Sasaki, J.; Aschmann, S. M.; Kwok, E. S. C.; Atkinson, R.; Arey, J. Products of the gas-phase OH and NO_3 radical-initiated reactions of naphthalene. *Environ. Sci. Technol.* **1997**, *31* (11), 3173−3179.

(14) Feilberg, A.; B. Poulsen, M. W.; Nielsen, T.; Henrik, S. Occurrence and sources of particulate nitro-polycyclic aromatic hydrocarbons in ambient air in Denmark. *Atmos. Environ.* **2001**, *35* (2), 353−366.

(15) Arey, J. Atmospheric reactions of PAHs including the formation of nitroarenes. *The Handbook of Environmental Chemistry PAHs and Related Compounds*; Springer-Berlag: Berlin, Germany, 1998, *3*, 347−385.

(16) Zimmermann, K.; Atkinson, R.; Arey, J.; Kojima, Y.; Inazu, K. Isomer distributions of molecular weight 247 and 273 nitro-PAHs in ambient samples, NIST diesel SRM, and from radical-initiated chamber reactions. *Atmos. Environ.* **2012**, *55* (0), 431−439.

(17) Dimashki, M.; Harrad, S.; Harrison, R. M. Measurements of nitro-PAH in the atmospheres of two cities. *Atmos. Environ.* **2000**, *34* (15), 2459−2469.

(18) Yaffe, D.; Cohen, Y.; Arey, J.; Grosovsky, A. J. Multimedia analysis of PAHs and nitro-PAH daughter products in the Los Angeles Basin. *Risk Anal.* **2001**, *21* (2), 275−294.

(19) Campbell, R. M.; Lee, M. L. Capillary column gas chromatographic determination of nitro polycyclic aromatic compounds in particulate extracts. *Anal. Chem.* **1984**, *56* (6), 1026−1030.

(20) Jinhui, X.; Lee, F. S. C. Quantification of nitrated polynuclear aromatic hydrocarbons in atmospheric particulate matter. *Anal. Chim. Acta* **2000**, *416* (1), 111−115.

(21) Schauer, C.; Niessner, R.; Poschl, U. Analysis of nitrated polycyclic aromatic hydrocarbons by liquid chromatography with fluorescence and mass spectrometry detection: air particulate matter, soot, and reaction product studies. *Anal. BioAnal. Chem.* **2004**, *378* (3), 725−736.

(22) Ringuet, J.; Leoz-Garziandia, E.; Budzinski, H.; Villenave, E.; Albinet, A. Particle size distribution of nitrated and oxygenated polycyclic aromatic hydrocarbons (NPAHs and OPAHs) on traffic and suburban sites of a European megacity: Paris (France). *Atmos. Chem. Phys.* **2012**, *12* (18), 8877−8887.

(23) Albinet, A.; Leoz-Garziandia, E.; Budzinski, H.; Villenave, E.; Jaffrezo, J. L. Nitrated and oxygenated derivatives of polycyclic aromatic hydrocarbons in the ambient air of two French alpine valleys: Part 1: Concentrations, sources and gas/particle partitioning. *Atmos. Environ.* **2008**, *42* (1), 43−54.

(24) Atkinson, R.; Aschmann, S. M.; Arey, J.; Barbara, Z.; Schuetzle, D. Gas-phase atmospheric chemistry of 1- and 2-nitronaphthalene and 1,4-naphthoquinone. *Atmos. Environ. (1967)* **1989**, *23* (12), 2679−2690.

(25) Feilberg, A.; Kamens, R. M.; Strommen, M. R.; Nielsen, T. Modeling the formation, decay, and partitioning of semivolatile nitro-polycyclic aromatic hydrocarbons (nitronaphthalenes) in the atmosphere. *Atmos. Environ.* **1999**, *33* (8), 1231−1243.

(26) Phousongphouang, P. T.; Arey, J. Rate constants for the photolysis of the nitronaphthalenes and methylnitronaphthalenes. *J. Photochem. Photobiol. A: Chem.* **2003**, *157* (2−3), 301−309.

(27) Feilberg, A.; Kamens, R. M.; Strommen, M. R.; Nielsen, T. Photochemistry and partitioning of semivolatile nitro-PAH in the Atmosphere. *Polycyclic Aromat. Compd.* **1999**, *14* (1−4), 151−160.

(28) Chapman, O. L.; Heckert, D. C.; Reasoner, J. W.; Thackabe, Sp. Photochemical studies on 9-nitroanthracene. *J. Am. Chem. Soc.* **1966**, *88* (23), 5550−5554.

(29) Crespo-Hernández, C. E.; Burdzinski, G.; Arce, R. Environmental photochemistry of nitro-PAHs: Direct observation of ultrafast

intersystem crossing in 1-nitropyrene. *J. Phys. Chem. A* **2008**, *112* (28), 6313−6319.
(30) Reichardt, C.; Vogt, R. A.; Crespo-Hernandez, E. On the origin of ultrafast nonradiative transitions in nitro-polycyclic aromatic hydrocarbons: Excited-state dynamics in 1-nitronaphthalene. *J. Chem. Phys.* **2009**, *131*, 22.
(31) Fan, Z.; Kamens, R. M.; Hu, J.; Zhang, J.; McDow, S. Photostability of nitro-polycyclic aromatic hydrocarbons on combustion soot particles in sunlight. *Environ. Sci. Technol.* **1996**, *30* (4), 1358−1364.
(32) García-Berríos, Z. I.; Arce, R. Photodegradation mechanisms of 1-nitropyrene, an environmental pollutant: The effect of organic solvents, water, oxygen, phenols, and polycyclic aromatics on the destruction and product yields. *J. Phys. Chem. A* **2012**, *116* (14), 3652−3664.
(33) Nielsen, T. Reactivity of polycyclic aromatic hydrocarbons towards nitrating species. *Environ. Sci. Technol.* **1984**, *18* (3), 157−163.
(34) Kautzman, K. E.; Surratt, J. D.; Chan, M. N.; Chan, A. W. H.; Hersey, S. P.; Chhabra, P. S.; Dalleska, N. F.; Wennberg, P. O.; Flagan, R. C.; Seinfeld, J. H. Chemical composition of gas- and aerosol-phase products from the photooxidation of naphthalene. *J. Phys. Chem. A* **2009**, *114* (2), 913−934.
(35) Thüner, L. P.; Bardini, P.; Rea, G. J.; Wenger, J. C. Kinetics of the gas-phase reactions of OH and NO_3 radicals with dimethylphenols. *J. Phys. Chem. A* **2004**, *108* (50), 11019−11025.
(36) Orzechowska, G. E.; Nguyen, H. T.; Paulson, S. E. Photochemical sources of organic acids. 2. Formation of C-5-C-9 carboxylic acids from alkene ozonolysis under dry and humid conditions. *J. Phys. Chem. A* **2005**, *109* (24), 5366−5375.
(37) United States Environmental Protection Agency: *Health and Environmental Effects Profile for Nitrobenzene*; Office of Solid Waste and Emergency Response: Washington, D.C. ECAO-CIN-P145. 1987.
(38) Gard, E.; Mayer, J. E.; Morrical, B. D.; Dienes, T.; Fergenson, D. P.; Prather, K. A. Real-time analysis of individual atmospheric aerosol particles: Design and performance of a portable ATOFMS. *Anal. Chem.* **1997**, *69* (20), 4083−4091.
(39) Zimmermann, R.; Ferge, T.; Galli, M.; Karlsson, R. Application of single-particle laser desorption/ionization time-of-flight mass spectrometry for detection of polycyclic aromatic hydrocarbons from soot particles originating from an industrial combustion process. *Rapid Commun. Mass Spectrom.* **2003**, *17* (8), 851−859.
(40) Silva, P. J.; Prather, K. A. Interpretation of mass spectra from organic compounds in aerosol time-of-flight mass spectrometry. *Anal. Chem.* **2000**, *72*, 3553−3562.
(41) Gross, D. S.; Galli, M. E.; Kalberer, M.; Prevot, A. S. H.; Dommen, J.; Alfarra, M. R.; Duplissy, J.; Gaeggeler, K.; Gascho, A.; Metzger, A.; Baltensperger, U. Real-time measurement of oligomeric species in secondary organic aerosol with the aerosol time-of-flight mass spectrometer. *Anal. Chem.* **2006**, *78* (7), 2130−2137.
(42) Gross, D. S.; Barron, A. R.; Sukovich, E. M.; Warren, B. S.; Jarvis, J. C.; Suess, D. T.; Prather, K. A. Stability of single particle tracers for differentiating between heavy- and light-duty vehicle emissions. *Atmos. Environ.* **2005**, *39* (16), 2889−2901.
(43) Baeza-Romero, M. T.; Wilson, J. M.; Fitzpatrick, E. M.; Jones, J. M.; Williams, A. In situ study of soot from the combustion of a biomass pyrolysis intermediate—Eugenol—and *n*-decane using aerosol time of flight mass spectrometry. *Energy Fuels* **2009**, *24* (1), 439−445.
(44) *Interpretation of Mass Spectra*, 4th ed.; McLafferty, F. W., Turecek, F., Eds.; University Science Books, 1993.
(45) van den Braken—van Leersum, A. M.; Tintel, C.; van 't Zelfde, M.; Cornelisse, J.; Lugtenburg, J. Spectroscopic and photochemical properties of mononitropyrenes. *Recl. Trav. Chim. Pays-Bas* **1987**, *106* (4), 120−128.
(46) Govindarajan, M.; Karabacak, M. FT-IR, FT-Raman and UV spectral investigation; computed frequency estimation analysis and electronic structure calculations on 1-nitronaphthalene. *Spectrochim. Acta Part A* **2012**, *85* (1), 251−260.
(47) Galloway, D. B.; Bartz, J. A.; Huey, L. G.; Crim, F. F. Pathways and kinetic energy disposal in the photodissociation of nitrobenzene. *J. Chem. Phys.* **1993**, *98* (3), 2107−2114.
(48) Berho, F.; Lesclaux, R. The phenoxy radical: UV spectrum and kinetics of gas-phase reactions with itself and with oxygen. *Chem. Phys. Lett.* **1997**, *279* (5−6), 289−296.
(49) Platz, J.; Nielsen, O. J.; Wallington, T. J.; Ball, J. C.; Hurley, M. D.; Straccia, A. M.; Schneider, W. F.; Sehested, J. Atmospheric chemistry of the phenoxy radical, C_6H_5O: UV spectrum and kinetics of its reaction with NO, NO_2, and O_2. *J. Phys. Chem. A* **1998**, *102* (41), 7964−7974.
(50) Jenkin, M. E.; Hurley, M. D.; Wallington, T. J. Investigation of the radical product channel of the $CH_3C(O)O_2 + HO_2$ reaction in the gas phase. *Phys. Chem. Chem. Phys.* **2007**, *9* (24), 3149−3162.
(51) Healy, R. M.; Hellebust, S.; Kourtchev, I.; Allanic, A.; O'Connor, I. P.; Bell, J. M.; Healy, D. A.; Sodeau, J. R.; Wenger, J. C. Source apportionment of PM2.5 in Cork Harbour, Ireland using a combination of single particle mass spectrometry and quantitative semi-continuous measurements. *Atmos Chem Phys* **2010**, *10* (19), 9593−9613.
(52) Bejan, I.; Abd El Aal, Y.; Barnes, I.; Benter, T.; Bohn, B.; Wiesen, P.; Kleffmann, J. The photolysis of ortho-nitrophenols: a new gas phase source of HONO. *Phys. Chem. Chem. Phys.* **2006**, *8* (17), 2028−2035.
(53) Clifford, G. M.; Hadj-Aïssa, A.; Healy, R. M.; Mellouki, A.; Muñoz, A.; Wirtz, K.; Martín Reviejo, M.; Borrás, E.; Wenger, J. C. The atmospheric photolysis of o-tolualdehyde. *Environ. Sci. Technol.* **2011**, *45* (22), 9649−9657.
(54) Brigante, M.; Charbouillot, T.; Vione, D.; Mailhot, G. Photochemistry of 1-nitronaphthalene: A potential source of singlet oxygen and radical species in atmospheric waters. *J. Phys. Chem. A* **2010**, *114* (8), 2830−2836.
(55) Sur, B.; Rolle, M.; Minero, C.; Maurino, V.; Vione, D.; Brigante, M.; Mailhot, G. Formation of hydroxyl radicals by irradiated 1-nitronaphthalene (1NN): oxidation of hydroxyl ions and water by the 1NN triplet state. *Photochem. Photobiol. Sci.* **2011**, *10* (11), 1817−1824.
(56) Gupta, P.; Harger, W. P.; Arey, J. The contribution of nitro- and methylnitronaphthalenes to the vapor-phase mutagenicity of ambient air samples. *Atmos. Environ.* **1996**, *30* (18), 3157−3166.
(57) Arey, J.; Atkinson, R.; Zielinska, B.; McElroy, P. A. Diurnal concentrations of volatile polycyclic aromatic hydrocarbons and nitroarenes during a photochemical air pollution episode in Glendora, California. *Environ. Sci. Technol.* **1989**, *23* (3), 321−327.
(58) Reisen, F.; Arey, J. Atmospheric reactions influence seasonal PAH and nitro-PAH concentrations in the Los Angeles Basin. *Environ. Sci. Technol.* **2005**, *39* (1), 64−73.